Chinese Chemical Letters 33 (2022) 3277–3280

Contents lists available at ScienceDirect

Chinese Chemical Letters

journal homepage: www.elsevier.com/locate/cclet

A BODIPY-modified polymeric micelle for sustaining enhanced photodynamic therapy

Yun-Chang Zhang[a,1], Lan She[a,1,*], Zi-Yue Xu[b,1], Ze-Kun Wang[b], Zhiqiang Ma[a], Feng Yang[a,*], Zhan-Ting Li[b,*]

[a] Department of Inorganic Chemistry, School of Pharmacy, Naval Medical University, Shanghai 200433, China
[b] Department of Chemistry, Shanghai Key Laboratory of Molecular Catalysis and Innovative Materials, Fudan University, Shanghai 200438, China

ARTICLE INFO

Article history:
Received 15 September 2021
Revised 20 October 2021
Accepted 1 November 2021
Available online 7 November 2021

Keywords:
Photodynamic therapy
Polymeric micelle
BODIPY
2-Pyridone
Tumor

ABSTRACT

Photodynamic therapy (PDT) has been gaining popularity in both scientific research and clinic applications due to its non-invasiveness and spatiotemporal targeting properties. Nevertheless, the local hypoxic microenvironment in tumor tissue impedes PDT universality. To overcome this drawback, a 2-pyridone-bearing BODIPY photosensitizer was synthesized rationally and introduced to polyethyleneglycol-*b*-poly(aspartic acid) to form a photosensitizer-$^1O_2$ generation, storage/release agent dual-loading system (PEG-*b*-PAsp-BODIPY). The investigation of the PDT effect at different illumination conditions *in vitro* and *in vivo* revealed that the system tremendously inhibited tumor proliferation, indicating that this new PEG-*b*-PAsp-BODIPY could act as a potentially effective photo therapeutic system for cancer therapeutics.

Photodynamic therapy (PDT) has attracted more and more attention due to its non-invasion and less drug resistance and high spatiotemporal precision versatile in cancer therapeutics [1–5]. PDT requires three elements, including photosensitizer, light and oxygen. The mechanism of PDT refers to the generation of reactive oxygen species (ROS, such as singlet oxygen $^1O_2$), by photosensitizer irradiation, resulting in tumor cells damage, apoptosis or even necrosis. However, the aggressive proliferation of tumor cells and the huge consumption of O_2 in PDT process aggravate tumor hypoxic microenvironments, which significantly limits the effect of PDT. Thus, the hypoxia of the tumor microenvironment (TME) is traditionally considered as the "Achilles heel" of PDT [6–11].

Various innovative strategies have been utilized to relieve the hypoxia in TME and boost the therapeutic effect of PDT. For examples, oxygen sufficient materials [12–14] and nanozymes [15–17] have been developed to generate oxygen in the TME. Recently, the 2-pyridone group has been attracted a considerable attention in photosensitizer modification, because it can react with $^1O_2$ to form 2-pyridone endoperoxides under light irradiation [18–24]. The endoperoxides formed can effectively release singlet oxygen by thermal cycloreversion *in vivo* under dark. Therefore, the fabrication of photosensitizers modified by the 2-pyridone group has a promising application for enhanced photodynamic therapy. Although inorganic nanomaterials have been widely used in photodynamic therapy, the metal ions of nanoparticles may cause acute toxicity and oxidative damage to main organs [20]. In contrast, organic polymer nanoparticles have advantages in structural stability and biocompatibility, at the same time, polymer nanoparticles could also prolong the blood circulation time, increase the cellular uptake and augment the therapeutic effect in intracellular level.

Herein, a new near-infrared photosensitizer BODIPY which bears a 2-pyridone group was synthesized. Considering the poor solubility of the photosensitizer in aqueous solution, we prepared a BODIPY-modified polymeric micelle complex from polyethylene glycol-*b*-poly(aspartic acid) and BODIPY *via* ester bond linkages, which was expected to improve the temporal and spatial regulation of photosensitizer bioavailability in the body. The polymer acts as a $^1O_2$ generation, storage and release unit that makes the system achieve efficient PDT with or without light irradiation.

The synthetic route of PEG-*b*-PAsp-BODIPY is shown in Scheme 1. All the compounds were characterized by nuclear magnetic resonance and electrospray ionization-mass spectrometry, which are provided in supporting information. BODIPY that bears two 2-pyridone groups, was chosen as the photosensitizer and $^1O_2$ storage/release agent. Polyethyleneglycol-*b*-poly(aspartic acid) (PEG-*b*-PAsp, DP $\approx$ 80, $M_w \approx$ 15,000), which was reported as pH responsive amphiphilic polymer [25,26], was introduced to increase water solubility, biocompatibility and EPR effect. Meanwhile, the BODIPY unit was bound to the PEG-*b*-PAsp by ester bonds to

* Corresponding authors.
E-mail addresses: slgs4100@126.com (L. She), yangfeng1008@126.com (F. Yang), ztli@fudan.edu.cn (Z.-T. Li).
[1] These authors contributed equally to this work.

https://doi.org/10.1016/j.cclet.2021.11.004
1001-8417/

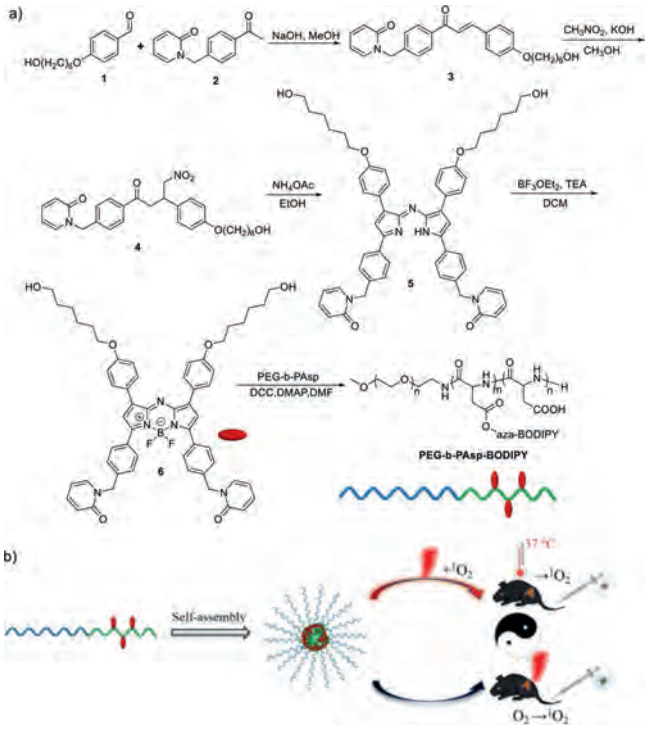

Scheme 1. (a) The synthetic route of PEG-*b*-PAsp-BODIPY. (b) Schematic illustration of PEG-*b*-PAsp-BODIPY for sustaining efficient PDT.

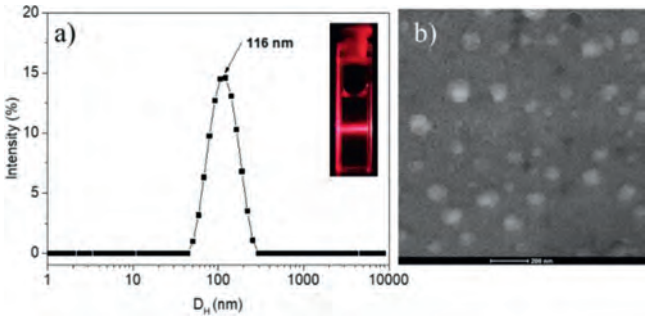

Fig. 1. (a) Hydrodynamic diameter distribution of PEG-*b*-PAsp-BODIPY (0.2 mg/mL) by DLS at pH 7.4 (inset: tyndall phenomenon of nano micelles in aqueous solution under laser irradiation). (b) TEM image of PEG-*b*-PAsp-BODIPY. Scale bar = 200 nm.

form the PEG-*b*-PAsp-BODIPY (45% m/m based on the BODIPY unit that was calculated by ^{1}H NMR, $M_w \approx 21{,}750$), which was expected to improve the stability of drugs during transportation.

The PEG-*b*-PAsp-BODIPY formed into nano micelles in aqueous solution by self-assemble and a distinct Tyndall Phenomenon was observed with a red laser beam through the solution (Fig. 1). The average hydrodynamic diameter of PEG-*b*-PAsp-BODIPY was about 120.3 nm that measured by dynamic light scattering (DLS). It could be observed that the PEG-*b*-PAsp-BODIPY exhibit a uniform spherical morphology with a diameter around 110 nm that was almost consistent with the diameter observed by DLS. Hydrodynamic stability of PEG-*b*-PAsp-BODIPY was also evaluated by diameter and PDI changes in 48 h after preparation (Fig. S10 in Supporting information), the results indicated the micelles could be stable in water. After laser irradiation with the diodelaser at 660 nm (Fig. S11 in Supporting information), the DLS result of PEG-*b*-PAsp-BODIPY that loading with $^1O_2$ was almost the same as before, demonstrating that loading with $^1O_2$ did not change the dispersity of the micelles in aqueous solution.

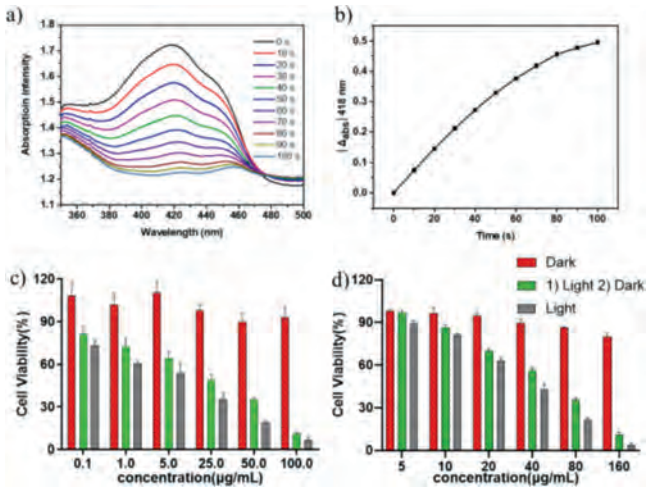

Fig. 2. (a) UV–vis absorption spectra of DPBF in water with PEG-*b*-PAsp-BODIPY (0.2 mg/mL) under 660 nm irradiation variation with time. (b) UV–vis absorption changes of DPBF at 418 nm. Cell viability of (c) B16-F10 and (d) A549 cells by CCK-8 assay after treated with different concentrations of PEG-*b*-PAsp-BODIPY at different conditions.

The photophysical properties of PEG-*b*-PAsp-BODIPY were investigated by UV–vis absorption and photoluminescence spectra. As exhibited in Fig. S12 (Supporting information), the absorption peaks of PEG-*b*-PAsp-BODIPY were located at 286 nm, 602 nm and 708 nm in water, which were consistent with the absorption of the samples that after 660 nm laser light irradiation. It meant that the material was negligibly affected by the $^1O_2$ loading. The maximum emission wavelength of BODIPY monomer centered at 720 nm (Fig. S13 in Supporting information), while PEG-*b*-PAsp-BODIPY in water exhibited no fluorescence which might be attributed to the aggregation-caused quenching [27,28].

To investigate the reliability of the continuous release of $^1O_2$ of PEG-*b*-PAsp-BODIPY, commercial singlet oxygen probe 1,3-diphenylisobenzofuran (DPBF) was employed as the probe [29,30]. As shown in Figs. 2a and b, the absorption at 418 nm decreased significantly as time went by, illustrating the oxidation of DBPF by the produced $^1O_2$ of this system.

The CCK-8 assay was measured to evaluate the inhibit activity of PEG-*b*-PAsp-BODIPY towards B16-F10 and A549 cells. Figs. 2c and d showed the cell viability at different concentrations of PEG-*b*-PAsp-BODIPY under light and dark conditions. It was evident that both the B16-F10 and A549 cells maintained a survival rate of more than 80% after 24 h of incubation with different doses of PEG-*b*-PAsp-BODIPY under dark condition, indicating that PEG-*b*-PAsp-BODIPY had good cytocompatibility. Under illumination conditions (660 nm, 0.2 W/cm^2), the cell survival rate obviously decreasesd with the increasing concentration of PEG-*b*-PAsp-BODIPY for both the B16-F10 and A549 cells. The half-maximal inhibitory concentration (IC_{50}) was calculated to be about 2.85 μg/mL (BODIPY = 1.3 μg/mL) for B16-F10, while the IC_{50} for A549 was about 29.88 μg/mL (BODIPY = 13.7 μg/mL). Furthermore, the PEG-*b*-PAsp-BODIPY was firstly under red light irradiation (660 nm) for 10 min, then incubated with the B16-F10 or A549 cells under dark condition, the cells also displayed relatively lower cell viability (IC_{50} according to BODIPY unit was 4.8 μg/mL for B16-F10 cells, while 31.1 μg/mL for A549 cells). All these results indicated that the PEG-*b*-PAsp-BODIPY could remarkably improve inhibitory efficacy for the proliferation of the tumor cells under illumination and dark condition.

From the confocal microscopy images (Fig. 3), it showed that the PEG-*b*-PAsp-BODIPY had excellent uptake and dispersity in B16-F10 and A549 cells. To investigate the ability of

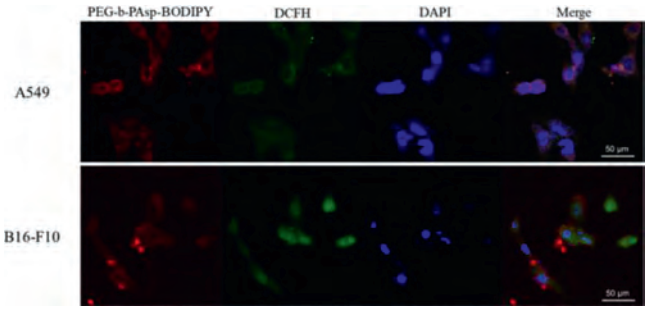

Fig. 3. Confocal microscopic images of intracellular ROS production. (a) A549 cells (up) and (b) B16-F10 cells (down) after incubation with PEG-*b*-PAsp-BODIPY under 660 nm irradiation at 37 °C. DCFH-DA was used as a ROS tracer probe, scale bar = 50 μm.

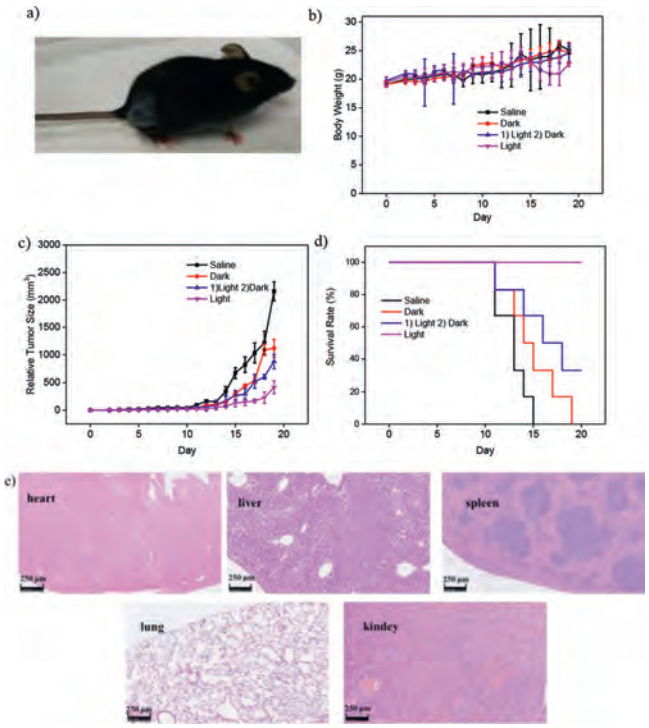

Fig. 4. (a) Photograph of a tumor-burdened mice. (b) Body weight changes, (c) relative tumor sizes and (d) survial curve of C57BL/6J male mice with different treatment. (e) H&E staining images of major organs (heart, liver, spleen, lung and kidney) for light irradiation group after 20 days treatment. Scale bar = 250 μm.

PEG-*b*-PAsp-BODIPY to generate singlet oxygen inside cell, 2′,7′-dichlorodihydrofluorescein diacetate (DCFH-DA) was used as a $^1O_2$ indicator [31]. The DCFH-DA could react with $^1O_2$ to transformed into DCF, which with green luminescence. When the B16-F10 cells were incubated with PEG-*b*-PAsp-BODIPY under red light irradiation (660 nm, 0.2 W/cm^2) for 10 min, there showed obviously green luminescence of DCF, indicating the generation of intracellular ROS of PEG-*b*-PAsp-BODIPY under illumination condition.

The photodynamic therapeutic effect of PEG-*b*-PAsp-BODIPY for the growth of B16-F10 melanoma was investigated with C57BL/6 J male mice (Fig. 4a). All mice received care in compliance with the guidelines outlined in the Guide for the Care and Use of Laboratory Animals. All procedures were approved by the Institutional Animal Care and Use Committee of the Naval Medical University. After the tumor tissues diameter increased around 0.4∼0.6 cm, 24 mice were randomly separated into four groups. The mice were injected with (1) saline, (2) PEG-*b*-PAsp-BODIPY without irradiation, (3) PEG-*b*-PAsp-BODIPY loading with $^1O_2$, (4) PEG-*b*-PAsp-BODIPY and irradiation, respectively. The weight of the mice were recorded during 20 days. From Fig. 4b, it did not show significant difference in average body weight of all groups during the treatment period, indicating excellent biocompatibility and low biotoxicity of PEG-*b*-PAsp-BODIPY *in vivo*. As shown in Figs. 4c and d, in comparison with the control groups, the tumor volumes changed little and the survival rate of mice extremely increased which treated with PEG-*b*-PAsp-BODIPY under irradiation. Meanwhile, an obvious inhibition on tumor growth was also observed in mice treated with PEG-*b*-PAsp-BODIPY under irradition and PEG-*b*-PAsp-BODIPY loading with $^1O_2$ under dark, indicating that the PEG-*b*-PAsp-BODIPY could achieve enhanced PDT performance by continuous generated $^1O_2$. Furthermore, to explore the phototoxicity of PEG-*b*-PAsp-BODIPY, the hematoxylin and eosin (H&E) analysis of the major organs (heart, liver, spleen, lung and kidney) was investigated. As shown in Fig. 4e, the PEG-*b*-PAsp-BODIPY exhibited no conspicuous tissue damage during the light irradiation therapeutic process, further confirming that the PEG-*b*-PAsp-BODIPY could be used as an efficient photodynamic therapeutic agent for cancer treatment.

In summary, a BODIPY-modified polyethyleneglycol-*b*-poly(aspartic acid) system (PEG-*b*-PAsp-BODIPY) was successfully prepared, which self-assembled into nano micelles in aqueous solution. The PEG-*b*-PAsp-BODIPY could act as a $^1O_2$ generation, storage and release phototherapeutic agent by introducing 2-pyridone to the BODIPY unit. The *in vitro* and *in vivo* experiment results demonstrated a good biocompatibility of PEG-*b*-PAsp-BODIPY, and the PEG-*b*-PAsp-BODIPY present enhanced photodynamic therapy effect and excellent tumor inhibition under illumination. Meanwhile, the polymer could persistently generate $^1O_2$ even at dark condition. Therefore, this work demonstrates the remarkable potential of PEG-*b*-PAsp-BODIPY in sustainable cancer photodynamic therapy in clinic. The fabrication and application of related photosensitive systems in tumor diagnosis and treatment will also be investigated in the future.

Declaration of competing interest

The authors declare that they have no known competing financial interests or personal relationships that could have appeared to influence the work reported in this paper.

Acknowledgment

This work was sponsored by Shanghai Sailing Program (No. 20YF1458000).

Supplementary materials

Supplementary material associated with this article can be found, in the online version, at doi:10.1016/j.cclet.2021.11.004.

References

[1] P. Agostinis, K. Berg, K.A. Cengel, et al., CA Cancer J. Clin. 61 (2011) 250–281.
[2] J.P. Celli, B.Q. Spring, I. Rizvi, et al., Chem. Rev. 110 (2010) 2795–2838.
[3] S.S. Lucky, K.C. Soo, Y. Zhang, Chem. Rev. 115 (2015) 1990–2042.
[4] Z.J. Zhou, J.B. Song, L.M. Nie, X.Y. Chen, Chem. Soc. Rev. 45 (2016) 6597–6626.
[5] X.S. Li, N. Kwon, T. Guo, Z. Liu, J.Y. Yoon, Angew. Chem. Int. Ed. 57 (2018) 11522–11531.
[6] W. Fan, P. Huang, X. Chen, Chem. Soc. Rev. 45 (2016) 6488–6519.
[7] M.L. Li, T. Xiong, J.J. Du, et al., J. Am. Chem. Soc. 141 (2019) 2695–2702.
[8] L.P. Zhao, R.R. Zheng, H.Q. Chen, et al., Nano Lett. 20 (2020) 2062–2071.
[9] L.Q. Li, C. Shao, T. Liu, et al., Adv. Mater. 32 (2020) e2003471.
[10] S.H. Qin, Y. Xu, H. Li, H.Y. Chen, Z.W. Yuan, Biomater. Sci. 10 (2022) 51–84.
[11] X.H. Zheng, L. Wang, Y.Y. Guan, et al., Biomaterials 235 (2020) e119792.
[12] F.M. Wei, T.W. Rees, X.X. Liao, L.N. Ji, H. Chao, Coordin. Chem. Rev. 432 (2021) e213714.
[13] P. Yuan, Z. Ruan, W. Jiang, et al., J. Mater. Chem. B 6 (2018) 2323–2331.
[14] S.N. Ma, J. Zhou, Y.X. Zhang, et al., ACS Appl. Mater. Inter. 11 (2019) 7731–7742.
[15] D.H. Hu, Z.W. Chen, Z.H. Sheng, et al., Nanoscale 10 (2018) 17283–17292.

[16] X.M. Zeng, S.Q. Yan, P. Chen, W. Du, B.F. Liu, Nano Res. 13 (2020) 1527–1535.
[17] J.T. Liu, L.Y. Ye, W.H. Xiong, et al., Chem. Commun. 57 (2021) 2820–2823.
[18] I.S. Turan, D. Yildiz, A. Turksoy, G. Gunaydin, E.U. Akkaya, Angew. Chem. Int. Ed. 55 (2016) 2875–2878.
[19] S. Ayan, G. Gunaydin, N. Yesilgul-Mehmetcik, et al., Chem. Commun. 56 (2020) 14793–14796.
[20] J.H. Zou, J.W. Zhu, Z. Yang, et al., Angew. Chem. Int. Ed. 59 (2020) 8833–8838.
[21] L. Jiao, X.Y. Zhang, J.N. Cui, X.J. Peng, F.L. Song, ACS Appl. Mater. Inter. 11 (2019) 25750–25757.
[22] W.Y. Xiao, P. Wang, C.J. Ou, et al., Biomaterials 183 (2018) 1–9.
[23] Y.Q. Li, C.C. Wang, L. Zhou, S.H. Wei, Chem. Commun. 57 (2021) 3127–3130.
[24] Y. Jing, Q. Xu, M. Chen, X.S. Shao, Bioorgan. Med. Chem. 27 (2019) 2201–2208.
[25] A.M. Eckman, E. Tsakalozou, N.Y. Kang, A. Ponta, Y. Bae, Pharm. Res. 29 (2012) 1755–1767.
[26] X.B. Xiong, Z. Binkhathlan, O. Molavi, A. Lavasanifar, Acta Biomater. 8 (2012) 2017–2033.
[27] C. Ren, H. Wang, D. Mao, et al., Angew. Chem. Int. Ed. 54 (2015) 4823–4827.
[28] Y. Zhu, W.H. Lin, W. Zhang, et al., Chin. Chem. Lett. 28 (2017) 1875–1877.
[29] T.F. Cui, J. Zhang, X.D. Jiang, et al., Chin. Chem. Lett. 27 (2016) 190–194.
[30] M.L. Agazzi, M.B. Ballatore, E. Reynoso, et al., Eur. J. Med. Chem. 126 (2017) 110–121.
[31] Z.Z. Wang, Y. Zhang, E.G. Ju, et al., Nat. Commun. 9 (2018) e3334.